Influence of the Number of Blades in the Power Generated by a Michell Banki Turbine

Yhon Castañeda Ceballos*, Mario Cardona Valencia**, Diego Hincapie Zuluaga***, Jorge Sierra Del Rio****, Sebastián Vélez García*****

*Instituto Tecnológico Metropolitano, Facultad de ingeniería, Former Student, 050034

**Instituto Tecnológico Metropolitano, Facultad de ingeniería, Professor, 050034

***Instituto Tecnológico Metropolitano, Facultad de ingeniería, Professor, 050034

****Instituto Tecnológico Metropolitano, Facultad de ingeniería, Professor, 050034

*****Instituto Tecnológico Metropolitano, Facultad de ingeniería, Professor, 050034

(yhoncastaneda187486@correo.itm.edu.co, maocarval@gmail.com, diegohincapie@itm.edu.co, jorgesierra@itm.edu.co, sebastianvelez@itm.edu.co)

‡ Corresponding Author; Jorge Sierra Del Rio, Calle 73 No. 76A - 354, Vía al Volador, Tel: +57 301 357 4232,

, jorgesierra@itm.edu.co

Received: 20.04.2017 Accepted:16.07.2017

Abstract- This article presents a computational simulation that studies the variation of power, depending on the number of blades in the runner. To develop the study, six CAD models were created using the software Solid Edge ST8, which comprises 16, 20, 23, 25, 28 and 32 blades, each corresponding to the volume of water taken into the turbine. The discretization of the control volume (water inside the turbine) was performed in the 'meshing' module Ansys® Workbench V17.0. The configuration of the equations that govern the fluid dynamics has been solved using Ansys CFX, where a model of homogeneous turbulence was used for the multiphase fluid (water-air), also a turbulence model that corresponds to k-ε for both phases was implemented, setting the next values as boundary conditions: a speed of 3.6 m/s in the nozzle, rotational speed of 450 RPM and atmospheric pressure at the outlet. There is an increment of the 3.2% in the power generated by Michell Banki turbine when the number of blades in the runner changes from 16 to 28.

Keywords Cross-Flow Turbine; Transient state; Ansys CFX 17.0; CFD analysis; Micropower

1. Introduction

1.1. Background

The sustainable development is based on three indispensable pillars that are the social and economic development and the natural environment protection. Climatic change and the exhaustion of non-renewable resources like coal, petroleum and natural gas are due to the accelerated growth of the electrical energy demand, and the big percent of non-interconnected zones (NIZ) existing nowadays, creating the need of searching new energy sources [1]. The study about renewable energy is taking a big impulse in many developed and underdeveloped countries, with the end of satisfying the electrical energy demand without causing a negative impact on the environment. The implementation of hydraulic turbines, especially the Michell Banki type cross-flow ones, allow supplying electrical energy to NIZ at a low installation and maintenance cost, improving these communities' quality of life. This turbine is used in micro-centrals, as it presents an efficient performance under flow variations and fabrication easiness [2].

A Michell Banki turbine, also known as the cross-flow turbine is a machine that takes advantage of the kinetic fluid energy and transforms it into rotational movement that at the same time is transferred to the axis of an electric generator, where the necessary electric fluid is obtained for the development of community daily activities. The power production starts in the nozzle, which transforms the pressure

energy in the inlet to kinetic energy (water jet). The water jet enters into the runner and transfers the energy in two stage. First, the water jet flows from outer part of the runner to the interior of it. this is considered as the first stage. Second, the water jet that travels from center to the outer is identified as the second stage, where finally the water is discharged. The first stage operates with a degree of reaction, due to the pressure exerted by the water to the runner blades. the water jet of the first stage travel to the second stage at atmospheric pressure, due to the presence of open space between stages, therefore The second stage operates on pure impulse principle [3]. Taking all the above into account the first stage provides a total of 70% of the energy and in the second stage is transferred the 30 % remaining. The energy transferred depend on the pressure load and friction stress at the surface of the blade. The reduction area due to the increment in the number of blades, generate a blocking in the fluid flow, increasing the energy losses by obstruction.

Based on OSSBERGER's original model, a similar design of the turbine is implemented, which is composed by four bodies: nozzle, runner, guide vane and casing as it is shown in Fig 1.

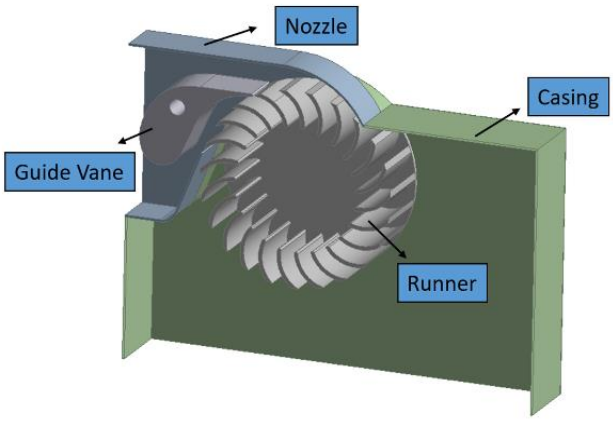

a) Michell Banki Turbine

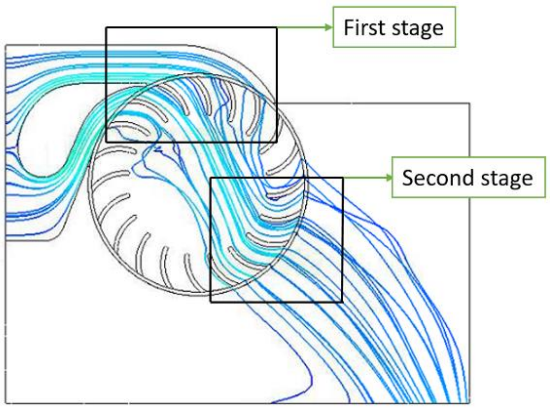

b) Energy transfer in the first stage and second stage

Fig. 1. Overview at cross flow Michell Banki Turbine

Table 1. Operating conditions

Parameter	Value
Rotational Speed (w)	450 RPM
Head (H)	10 m
Discharge (Q)	0.148 m3/s

For the design process of the Michell Banki turbine, the Head and discharge are required to start the art. With this information and given the relation $Q/\sqrt{H}$ the specific discharge value is calculated and the runner's diameter is selected through standardized tables. The geometry of the nozzle must considerate a good fluid conduction and acceleration, as well as the regulation of this fluid toward the blades of runner. The width of the nozzle is given by equation (1).

$$B = \frac{0.96Q}{D_e\sqrt{H}} \quad (1)$$

Where B is the width of the nozzle and D_e is the external diameter of the runner.

1.2. Previous works

In literature, the results of experimental and numerical studies, related to the determination of the generated power in the cross-flow turbines by variating the blade's quantities that compose the runner can be found.

Nadim M. Aziz and Venkappayya R. Desai [4] investigated experimentally the influence in the efficiency of the number of blades in the runner of cross-flow turbine. The authors found that the maximum efficiency is reached by the configuration of a runner with 25 blades. Experiments done by Aziz and Totapally [5] found that the number of blades in the runner of a Michell Banki turbine can vary from 15 to 35, the study showed that the maximum efficiency is found in a runner of 30 blades. An investigation done by H. Olgun and A. Ulkun [6] shows the configuration of a runner of the Michell Banki turbine with 20, 24, 28 and 32 blades, the authors found an efficiency of 73%, being this one the maximum that is achieved with a configuration of 28 blades in the runner. Choi, et al. [7] performing a numerical study found that the maximum efficiency for a cross-flow turbine is shown by a runner with 30 blades, finding a similar result to Aziz and Totapally's study. Vincenzo Sammartano, et al. [8] performed a steady state-3D CFD (Computational Fluid Dynamic) simulation for three Michell Banki runners designed with 30, 35 and 40 number of blades, in this study, the blade profile has a knife border attack as well as at the end of the profile geometry. The authors determined that an increase of the blades' number in the runner of a Michell Banki turbine, raises its performance, finding a maximum of 35 blades for a 22° attack angle. Furthermore, the authors argue that a runner with more than 35 blades, presents a

considerable restriction to the water flow, causing a loss of power generated in the runner. Additionally, it is possible that not considerate a thickness border attack at the blade profile, could increase cross flow area, for this reason, a decrease of the flow restriction and increase the optimal number of blades at the runner turbine respect to the others references. Nirmal Acharya, et al. [9] conducted a transient CFD simulation in the Ansys CFX V13 commercial software for a Michell Banki turbine varying the geometrical configurations like nozzle shape, guide vane angle and the number of blades, in this study, 8 configurations for the runner were performed correspond to 16, 18, 20, 22, 24, 26, 28 and 32 blades, the authors found that the highest power of the turbine corresponds to the runner turbine configuration with 26 blades. Shashank Mani, et al. [10] studied numerically different runner configurations, varying the numbers of blades by 18, 22, 26 and 30 blades for discharges of 0.3 m3/s, 0.4 m3/s and 0.48 m3/s. According to the authors, the efficiency increases 3.2% when the number of blades in the runner varies from 18 to 22. As opposed to other authors which present a higher number of blades like the best runner configuration.

The table 2 summaries the numerical and experimental available results in the literature, highlighting the influence of the number of blades on runner in the hydraulic efficiency at the Michell Banki turbine.

Table 2. Resume of state of the art

Authors	Quantity of studied blades	Optimum quantity of blades	Reference
V. Sammartano, et al.	30, 35, 40	35	[8]
Y. D Choi, et al	N/A	30	[7]
Aziz, N.M. and Totapally, H.G.S	15 - 35	30	[5]
H. Olgun and A. Ulkun	20, 24, 28, 32	28	[6]
Nadim M. Aziz and Venkappayya R. Desai	N/A	25	[4]
Shashank Mani, et al.	18, 22, 26, 30	22	[10]
N. Acharya, et al.	16, 18, 20, 22, 24, 26, 28, 32	22	[9]

According to the state of art related to the desired quantity of blades at the Michell Banki runner, it is possible to summarize that there is a big range (20 to 30 blades) for the optimal number of blades, in order to obtain the higher efficiency in the turbo-machine.

The main objective of this study is to numerically determine the optimal number of blades that compose the runner in order to obtain the highest efficiency for the turbine at constant operating conditions. Six alternatives of the runner are presented, which are composed by 16, 20, 23, 25, 28 and 32 blades for a turbine operating under the conditions described in Table 1. Transient numerical simulation was developed in the module CFX of the software ANSYS V17.0. Where were considered the configurations showed before, obtaining the generated power and the incidence of the blades' number in the turbomachine's efficiency per each case.

2. Methodology

2.1. Control Volume

The geometrical design corresponds by OLADE empirical correlations [11] and the model was designed in the Software Solid Edge ST8, where the construction is done through basic operations to generate the volume in the parts. The fluid input region is in the nozzle, and the guide vane is inside of it, always in the same position, which oversees the control of the fluid quantity that gets into the runner. These two parts are assembled together with the casing and the runner, using methods of relation in the same software. Finally, different runners are done by variating the number of

blades that compose it, obtaining 6 models configured with 16, 20, 23, 25, 28 and 32 blades.

Once the pieces are built and assembled, the next step is the control volume extraction by Booleans operations, which is composed by the fluid volume inside the turbine, 6 control volumes are obtained and correspond to the 6 models with variations in the number of blades. Figure 2 shows a ring volume domain performed in order to simplify the interfaces configurations at the boundary conditions.

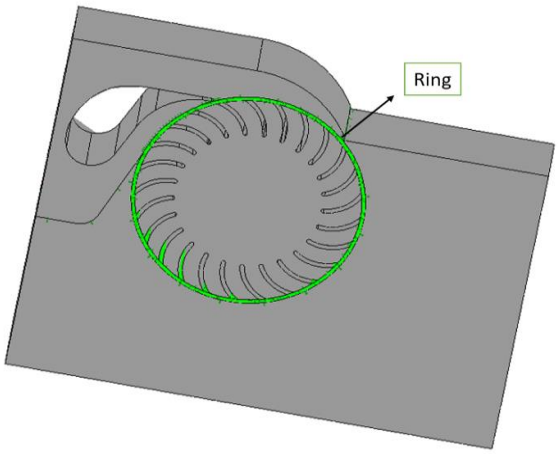

Fig. 2. Ring volume at Michell Banki Turbine.

2.2. Discretization and boundary conditions

The discretization of the turbine's control volume was done in the 'Meshing' module of the software ANSYS V17.0, where tetrahedral elements are implemented, which compose the fluid volume inside the turbine. Around twenty millions of elements (20e6) were used in the discretization process to achieve an independence of the mesh respect to the torque generated at the output shaft, presenting statistics of maximum obliquity in the mesh of 0.80, an aspect relation of 10.3, a minimum orthogonal quality of 0.23 and an element minimum quality of 0.21, all this is to ensure a decrease of the measurement error by discretization in the reply value, corresponding to a variation below 2% of the generated torque.

A study of grid independence for different configurations in the runner with 28 blades of Michell Banki turbine were performed. Five different meshes were applied starting with 3.4 up to 50 million number of cells. The resultant torque achieved is shown in Fig 3 for each case. In that way were possible to determinate that the error rate is approximately 2% for the grid number 3.

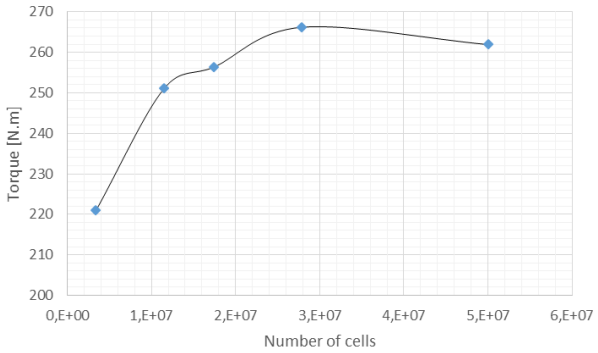

Fig. 3. Grid independence study for the runner with 28 blades

The boundary conditions associated to the control volume are shown in Fig. 4, which corresponds to the operations conditions showed in table 1. The velocity inlet of 3.2 m/s at inlet nozzle corresponding to the operating discharge. A rotating domain with velocity rotational speed of 450 RPM about "Y" axis of the Cartesian coordinate system is established for the runner. A subsonic flow regime (Ma<1), a relative pressure of zero (0) Pa, and a volumetric fraction for both fluids (water-air) of zero gradient are configured for the opening boundary condition. Non-sliding walls are configured for each domain corresponding to blades at the runner and casing turbine. The interfaces boundary conditions existing between the rotating-static domains. In this study two interfaces were established. The first interface is given between the nozzle, ring and casing, a 'fluid-fluid'-type interface is implemented for it, where the ring region that limits with the other domains (casing and nozzle) are specified later, and the regions of the casing and nozzle that limit with the ring are selected equally, then an interface model is implemented and configured as 'general connection' and finally, as none of the named domains rotate about each other, then there is no Mix/Change model. The second interface is between the ring and the runner, where like the first interface, a 'fluid-fluid'-type interface is set too, and all the regions in which every domain (ring and runner) limit between each other are selected too. Also, the interface model is set as 'general connection', but unlike the first interface, this one has domain moving, which is the runner, then the framework of Mix/Change models is set as 'Transient runner stator' due to the transient conditions in the fluid between nozzle and the runner.

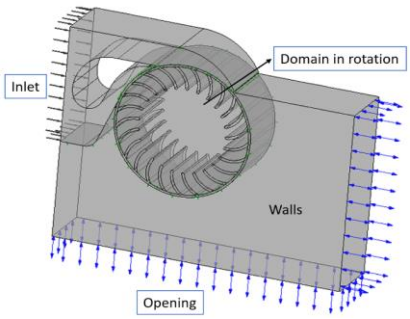

a) Boundary condition

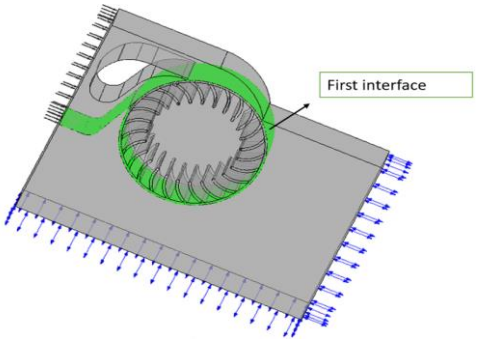

b) Interface between nozzle, casing and ring

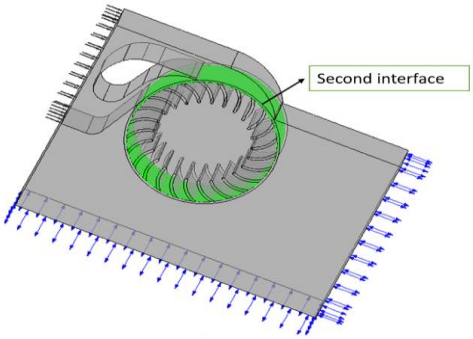

c) Interface between ting and runner

Fig. 4. Boundary condition and domains interfaces in the numerical simulation.

2.3. Numerical method

Ansys, inc. is a commercial software highly used at industrial and academic projects. Ketan Ajay and Lal Kundan carried out a CFD simulation in Ansys Fluent 14.5, where is modelled a solar flux through solar load cell [12]. Mukesh M. Yelmule and EswaraRao Anjuri realized a computational prediction of NREL Phase VI rotor for a wind turbine with power rating of 20kW. The authors carried out all the CFD simulations in Ansys CFX 12.1 [13]. Rami Elnoumeir, et al. developed a numerical study of a Honeycomb Solar Receivers. They said that a numeric prediction of the heat transfer and flow properties are useful for optimize the components of Honeycomb Solar Receivers. The authors used Ansys to compute the effective extinction coefficient of the solar radiation [14].

The CFD simulation is a process applied to study hydraulic performance of turbo-machine, since it is effective in time management [15]. The aerodynamics profiles at the runner are related to the turbine efficiency. Authors as Onur GUNEL, et al. used CFD analysis for aerodynamic performance using Ansys-Fluent. This software solves the RANS equations using finite volume discretization [16]. Emre KOC, et al. performed a CFD methods for study the aerodynamic performance of a wind turbine, where they monitoring power and torque curve of the hydraulic turbine [17]. Kazuyuki NAKAMURA, et al. study the hydraulic performance in a high head Francis turbine. They were using CFD for cover the operation of a Francis turbine, where RNG k-ε turbulence model was applied; this has accuracy in prediction in the operation of turbo-machines [18]. Other investigation developed by S. Yamamoto, et al. employed a 3D-CFD code KIVA-3V for simulate the disintegration, collision, combustion of droplets in a combustion chamber [19].

The solution process of the equations of momentum and mass conservation was done using the CFX module of Ansys Workbench V 17.0. A method of implicit solution of Roe-FDS flow-type and second-order spatial discretization guarantee a reliable solution. The properties of the biphasic fluid were established for water and air at 25°C with a reference pressure of 1 atm for the fluid's volume, because the turbine's operating conditions do not manage to generate changes in both fluid's density, which are considered of continuous phase and with stress between fluids, characterized by a superficial tension coefficient of 73.5 dyna cm^{-1}. The implemented turbulence model corresponds to k-ε for a simulation in transitory state with a time-step of 0.01 s for a total simulation time of 1 s. Based on the residues obtained by the root mean square (RMS) of 1e-4, and the monitoring of every time-step of the generated torque, the convergence criteria established for the simulation control were set, and guaranteed a reliable simulation response. The CFD simulation process was done in a high speed computer (cluster) of the Technological Metropolitan Institute from Medellín-Colombia, which is composed by the operating system Windows Server 2008 R2, and has a processing capacity of 32 cores and a RAM of 256 GB. In Table 3, the simulation times for each model can be observed with the runner's different configurations.

Table 3. Simulation time for each model

Michell Banki turbine's model	Number of blades in the runner	Simulation time [hours]
1	16	26
2	20	41
3	23	80
4	25	176
5	28	27
6	32	60

2.3.1. Fundamental equations

One of the most well-known turbulence models is the k-epsilon model, where 'k' is the turbulent kinetic energy and is defined as the variance of the fluctuations in the speed. It has some dimensions of (L^2 /T^2), ε is the dissipation of the turbulence of Eddy (the velocity in which the velocity fluctuations dissipate), and has some dimensions of k per unit of time (L^2/T^3).

The k-ε model introduces two new variables in the system of equations. The equation of continuity is defined by (2):

$$\frac{\partial \rho Ui}{\partial t} + \frac{\partial}{\partial x_i}(\rho U_i) = 0 \tag{2}$$

The equation of momentum is:

$$\frac{\partial \rho Ui}{\partial t} + \frac{\partial}{\partial x_i}(\rho U_i U_j) = -\frac{\partial p'}{\partial x_i} + \frac{\partial}{\partial x_j}\left[\mu_{eff}\left(\frac{\partial U_i}{\partial x_j} + \frac{\partial U_j}{\partial x_i}\right)\right] + S_M \tag{3}$$

Where S_M is the sum of the body forces, μ_{eff} is the Effective Viscosity that represents the turbulence, p' is a modified pressure.

The k-ε model, like the model of the zero equation, is based on the Eddy's viscosity concept, defined by equation (4).

$$\mu_{eff} = \mu + \mu_t \tag{4}$$

Where μ_t correspond to the turbulence viscosity. The k-ε model assumes that the turbulence viscosity is linked to the kinetic energy and the turbulence's dissipation through the equation (5).

$$\mu_t = C_\mu \rho \frac{k^2}{\varepsilon} \tag{5}$$

Where C_μ is a constant. The values of k and ε come directly from the differential transport equations for the turbulence's kinetic energy and dissipation rate defined by equation (6):

$$\frac{\partial(\rho k)}{\partial t} + \frac{\partial}{\partial x_j}(\rho U_j k) = \frac{\partial}{\partial x_j}\left[\left(\mu + \frac{\mu_t}{\sigma_k}\right)\frac{\partial k}{\partial x_j}\right] + P_k - \rho\varepsilon + P_{kb} \frac{\partial(\rho\varepsilon)}{\partial t} + \frac{\partial}{\partial x_j}(\rho U_j \varepsilon) = \tag{6}$$
$$\frac{\partial}{\partial x_j}\left[\left(\mu + \frac{\mu_t}{\sigma_\varepsilon}\right)\frac{\partial \varepsilon}{\partial x_j}\right] \frac{\varepsilon}{k}\left(C_{\varepsilon 1} P_k - C_{\varepsilon 2}\rho\varepsilon + C_{\varepsilon 1} P_{sb}\right)$$

Where $C_{\varepsilon 1}$, $C_{\varepsilon 2}$, σ_k and σs are constants.

The torque generated by turbine Michell Banki is calculated with the equation (7), where S represents the surfaces comprising all rotating parts, $\hat{n}$ is a unit vector normal to the surface, $\vec{r}$ is the position vector, $\hat{a}$ is a unit vector parallel to the axis of rotation and $\overline{\overline{\tau}}$ (the total stress tensor) that uses the continuum mechanics to model the part of the stress at any point in some material. See guide of modeling of CFX of ANSYS® [20].

$$T = \left[\int_S (\vec{r} \times (\overline{\overline{\tau}} \cdot \hat{n}))dS\right] \cdot \hat{a} \tag{7}$$

The turbine efficiency is calculated through the equation (8), defined as the relation between the output power in the axis defined as, $P_{out} = T * w$, the available power in the input of the turbo-machine is defined as $Pin = \gamma * Q * H * \eta$ which is calculated using the following correlation:

$$\eta = \frac{T * w}{\gamma * Q * H} \tag{8}$$

where T is the Torque $[Nm]$ generated in the output Shaft of the turbine, water specific weight $\gamma = \rho g$, w, Q and H as the operations conditions defined in the Table 1.

3. Results and Discussion

Figure 5 presents the variation of the generated power and efficiency in the Michell Banki turbine depending on the number of blades. For this investigation were found that the increase of blades in the runner generates an increase in the turbine's power. This is shown in the power generation for the runner configuration by 16 up to 28 blades, the relation between the capacity of energy transfer and the reduction of cross flow area due to the increment of the number of blades, which increase the blocking fluid flow, therefore is reached the best configuration with 28 blades. Thus, the maximum output power of 12.54 kW with an efficiency of 86%. This phenomenon shows up due to the separation between blades in the runner. Allowing a good energy transference from the fluid to the runner at the first and second stage for a minimum energy loss by blockage for the fluid flow. The runner configured with 32 blades, presents a decrease in the generated power of 14.6% respect to the configuration with 28 blades, on account of decreasing of the relation between the energy transferred and the loss of energy by blockage of the fluid flow respect to the case of 28 blades.

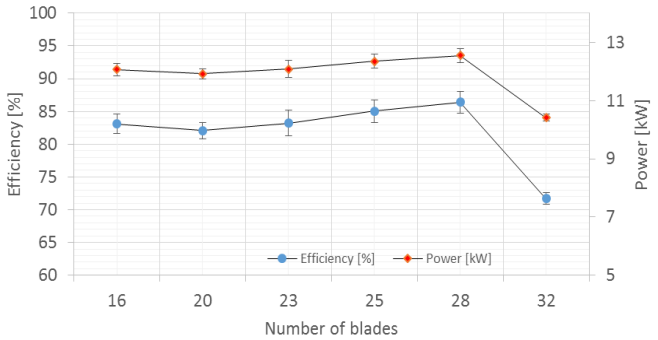

Fig. 5. Power (kW) and efficiency (%) with the variation in number of blades.

Figure 6 shows the comparison between the present work with numerical and experimental results showed before in previous works. It is possible to determine that the optimal number of blades is between 23 and 30 blades, where the blade's profile plays a big role in the optimal number of blades due to the hydrodynamic efficiency and the fluid blade interaction. The results of the present simulation are in accord to the experimental study performed by H. Olgun and A. Ulkun [6], where a Michell Banki turbine, set with 28 blades like the optimal number of blades with an efficiency of 73%.

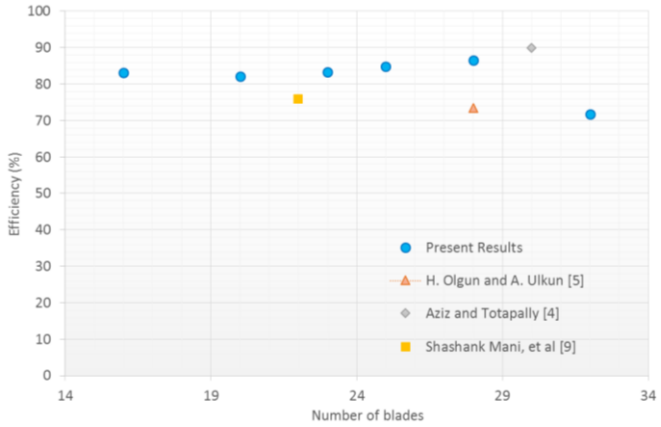

Fig. 6. Comparisons of the efficiency against the number of blades by different references.

The difference at efficiencies values corresponds to the variation in geometry configurations at each model studied, mainly in the injector design and ratio between the external and internal diameter of the runner turbine. Also, Aziz and Totapally [5], Y. D Choi et al. [7] results presents similar trend. Differences between the present simulation and the numerical results presented by N. Acharya, et al. [9], Shashank Mani, et al [10], V. Sammartano, et al. [8], in others, were found too, this is because of the difference in the blade's profile used in each study.

Figure 7 shows the water volume fraction, pressure contour and velocity streamline for the cases with 23, 28 and 32 blades at the symmetry plane, where the trajectory followed by the fluid can be seen from the inlet to the output (left to right in the picture). In the second column of the figure the water volume fraction contours can be analyzed, for each case, the ratio between the water volume caught inside the runner and the total runner volume were calculated in order to determine the blockage of the fluid flow. Thus, it is possible to observe that the higher quantity of water caught inside the runner is associated with the case with 32 blades with a 48.64%. By the other hand, the lower quantity of water caught inside corresponds to the case with 28 blades with a 41.92%. Finally in middle is the case with 23 blades with a 44.63%.

No. of blades	Water volume fraction	Velocity streamlines	Pressure contour
23	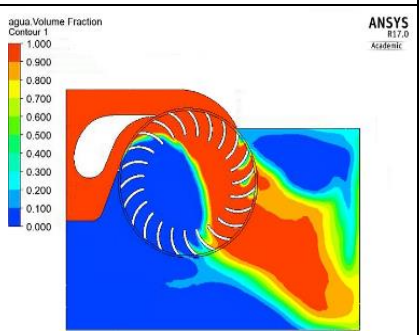	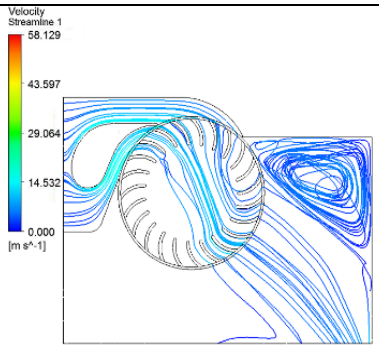	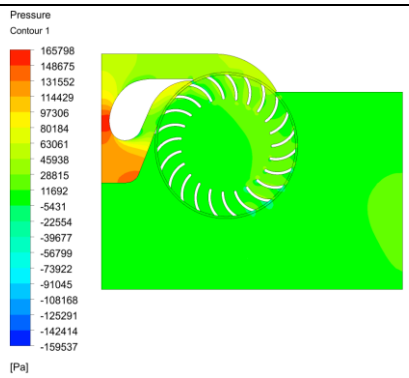
28	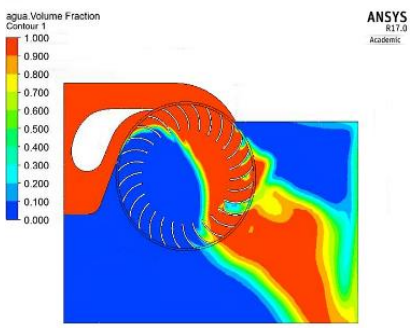	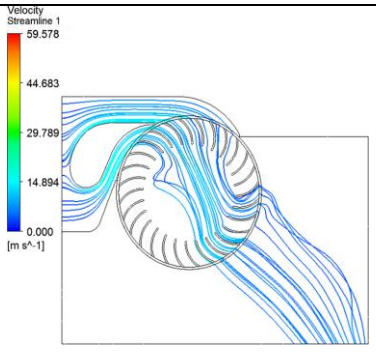	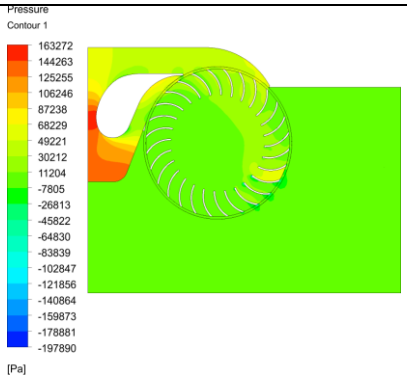

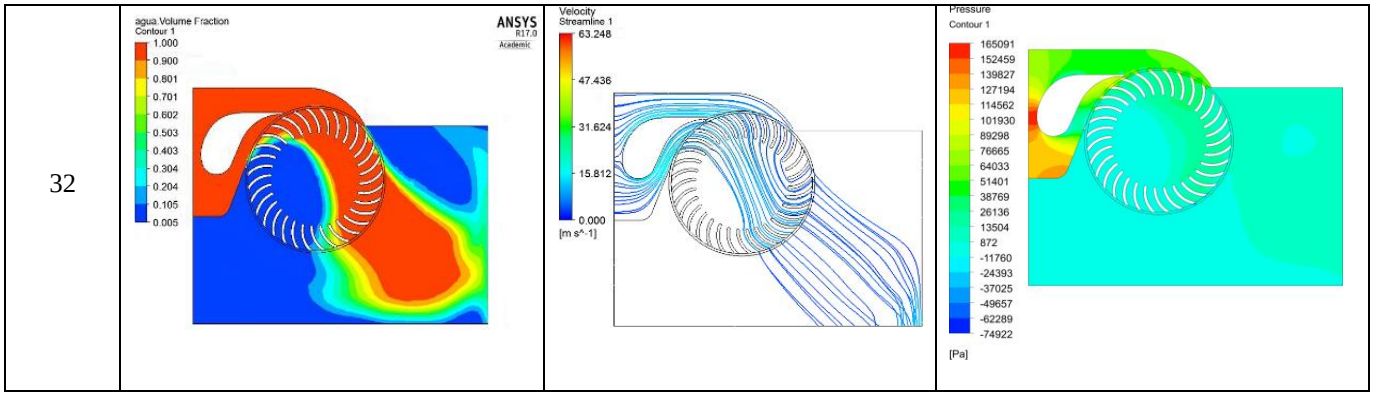

Fig. 7. Water Volume Fraction, velocity streamlines and pressure contour at symmetry plane of the turbine

To summarize, a higher value of water caught shows how the obstruction to fluid flow reduces the efficiency of the turbine. The last column shows a pressure contour at the symmetry plane produced by the fluid flow, when it travels through the turbine since the inlet to the outlet (opening), the value associated to the red color indicates the maximal pressure generated by the water and it is observed on the inlet (Nozzle guide vane), while the blue color represents a vacuum pressure, which these turbine models don't present. The highest difference of pressure between the concave and convex sides of the blades is reached for the case with 28 blades, extracting in that way a higher quantity of energy from the fluid in comparisons with the other cases, due to of tendency to rotate is produced by the pressure difference between the both sides of the blade. The third column shows the streamlines of fluid flow. The velocity streamline shows the water velocity in different points of the turbine. For the first model configured with 23 blades is appreciated a phenomenon that consists in the water recirculation, it presents a power loss in the turbine. The turbine configured with 28 blades presents a water high speed in the runner, therefore the fluid gives greater kinetic energy in the second stage, unlike the turbine configured with 32 blades, which fluid motion obstruction produces power loss in the second stage.

4. Conclusions

The increase of the efficiency was found when the turbomachine's runner is configured with 28 number of blades, as can be seen in Fig. 4, brings as consequence an increase in the power generated by the turbine, in this way the operation rank of the turbine can be bigger and will help to compensate those populations with a high demand of electrical energy. The CFD analysis applied in the investigation shows results with great accuracy that can be compared with real experiments, which allows the results of the fluids computational analysis to be reliable.

To obtain the behavior of the power with respect to the number of blades in each model of the configured turbine, the implementation of a numerical analysis of transitory state was necessary in CFD, which is a tool that allows to analyze volumetric fractions, velocity profiles, torques and others. The reliability of the results obtained by these analyses carried out in the software ANSYS V17.0, depends on the discretization of each configured model's control volume.

Further work

The number blades optimum change with the hydrodynamic profile, therefore will be carried out a study of the hydrodynamic profile's incidence in the power generated for a number of blades between the ideal range 23 to 30 blades.

References

[1] N. Unidas and D. Sostenible, "La sostenibilidad del desarrollo a 20 años de la Cumbre para la Tierra: Avances, brechas y lineamientos estratégicos para América Latina y el Caribe," 2012.

[2] Andrade JD, Curiel C, Kenyery F, Aguillon O, Vasquez A, Asuaje M. Numerical investigation of the internal flow in a Banki turbine. Int J Rotating Mach 2011; 12:841214.

[3] C. S. Kaunda, C. Z. Kimambo, and T. K. Nielsen, "A numerical investigation of flow profile and performance of a low cost Crossflow turbine," vol. 5, no. 3, pp. 275–296, 2014.

[4] Nadim M. Aziz and V. R. Desai, "An Experimental Study of the Effect of Some Design Parameters in Cross-Flow Turbine Efficiency", Engineering Report, Department of Civil Engineering, Clemson University, 1991.

[5] Aziz, N.M.; Totapally, H.G.S. Design Parameter Refinement for Improved Cross Flow Turbine Performance. In Engineering Report, Departement of Civil Engineering, Clemson University, Clemson, SC, USA, 1994.

[6] H. Olgun and A. Ulku. A study of cross-flow turbine – effects of turbine desing parameters on its performance. Department of mechanical engineering, University of Karadeniz Technical, Trabzon, 2884 – 2838.

[7] Y D Choi, H Y Yoon, M Inagaki, S Ooike, Y J Kim and Y H Lee, Performance improvement of a cross-flow hydro turbine by air layer effect. IOP Publishing, doi:10.1088/1755-1315/12/1/012030.

[8] Vincenzo Sammartano, Costanza Aricò, Armando Carravetta, Oreste Fecarotta and Tullio Tucciarelli. Banki-Michell Optimal Design by Computational Fluid Dynamics Testing and Hydrodynamic Analysis. Energies (2013), 6, 2362-2385.

[9] Nirmal Acharya, Chang-Gu Kim, Bhola Thapa y Young-Ho Lee. Numerical analysis and performance enhancement of a cross-flow hydro turbine. Renewable Energy 80 (2015) 819-826.

[10] S. Mani, P. K. Shukla, C. Parashar, and P. G. Student, "Effect of Changing Number of Blades and Discharge on the Performance of a Cross-Flow Turbine for Micro Hydro Power Plants Depart ment of Civ il Engineering," Int. J. Eng. Sci. Comput., 2016.

[11] Hernández B. Carlos A. Diseño y Estandarización de Turbinas Michell-Banki. OLADE (Organización latinoamericana de Energía). 1980, 2-21.

[12] K. Ajay and L. Kundan, «Experimental and CFD Investigation on the Efficiency of Parabolic Solar Collector Involving Al2O3/H2O (DI) Nanofluid as a Working Fluid,» *INTERNATIONAL JOURNAL of RENEWABLE ENERGY RESEARCH*, vol. 6, nº 2, pp. 392-401, 2016.

[13] M. M. Yelmule and E. Anjuri VSJ, «CFD predictions of NREL Phase VI Rotor Experiments in NASA/AMES Wind tunnel,» *INTERNATIONAL JOURNAL of RENEWABLE ENERGY RESEARCH*, vol. 3, nº 2, pp. 261-269, 2013.

[14] R. Elnumeir, R. Capuano and T. Fend, «Numerical Evaluation of the Extinction Coefficient,» *INTERNATIONAL JOURNAL OF RENEWABLE ENERGY RESEARCH*, vol. 7, nº 1, pp. 411-421, 2017.

[15] D. Sarper Semerci and T. Yavuz, «Increasing Efficiency of an Existing Francis Turbine by Rehabilitation Process,» *5th International conference on Renewable Energy Research and Application.* DOI: 10.1109/ICRERA.2016.7884440, pp. 107-111, 2016.

[16] O. GÜNEL, E. KOÇ and T. YAVUS, «CFD vs. XFOIL of Airfoil Analysis at Low Reynolds,» *5th International conference on Renewable Energy Research and Application.* DOI: 10.1109/ICRERA.2016.7884411, pp. 628-632, 2016.

[17] E. KOÇ, O. GÜNEL and T. YAVUZ, «Comparison of Qblade and CFD Results for Small-Scale Horizontal Axis Wind Turbine Analysis,» *5th International conference on Renewable Energy Research and Application.* DOI: 10.1109/ICRERA.2016.7884538, pp. 204-209, 2016.

[18] K. NAKAMURA, T. SHIGENOBU, S. HARADA and T. MURAKI, «High Head Pumped Storage Power Plant,» *5th International conference on Renewable Energy Research and Application.* DOI: 10.1109/ICRERA.2012.6477312, pp. 1-6, 2012.

[19] S. Yamamoto, D. Sakaguchi, H. Ueki and M. Ishida, «Effect of Fuel Mass Distribution on Ethanol,» *5th International conference on Renewable Energy Research and Application.* DOI: 10.1109/ICRERA.2012.6477397, pp. 1-6, 2012.

[20] C. Ansys, "ANSYS CFX-solver theory guide," ANSYS CFX Release, vol. 15317, no. April, pp. 724–746, 2009.